

Ranges of Peak Storm Tides Between Open-Coast and Bay Locations

**Key Points:**

- The range of peak storm tides can be larger at inland locations than at the open coast
- The wind intensity and storm track are significant contributors to the range of possible storm tides
- Specific storms may still cause a larger peak storm tide at the open coast

Correspondence to:

J. S. Knowles,
jsknowle@ncsu.edu

Citation:

Knowles, J. S., Dietrich, J. C., Elkut, A. E., Puleo, J. A., Shi, F., & Tateosian, L. G. (2025). Ranges of peak Storm tides between open-coast and Bay locations. *Journal of Geophysical Research: Oceans*, 130, e2025JC023158. <https://doi.org/10.1029/2025JC023158>

Received 11 JUL 2025

Accepted 17 OCT 2025

Author Contributions:

Conceptualization: Jenero S. Knowles, J. C. Dietrich

Data curation: Jenero S. Knowles, J. C. Dietrich, A. E. Elkut, J. A. Puleo, F. Shi

Formal analysis: Jenero S. Knowles, J. C. Dietrich, A. E. Elkut, J. A. Puleo, F. Shi

Funding acquisition: J. C. Dietrich, J. A. Puleo

Investigation: Jenero S. Knowles, J. C. Dietrich




Methodology: Jenero S. Knowles, J. C. Dietrich, A. E. Elkut, J. A. Puleo, F. Shi

Project administration: J. C. Dietrich, J. A. Puleo

Resources: Jenero S. Knowles, J. C. Dietrich, A. E. Elkut

Software: Jenero S. Knowles, J. C. Dietrich

Supervision: J. C. Dietrich

Jenero S. Knowles¹ , J. C. Dietrich¹, A. E. Elkut², J. A. Puleo² , F. Shi² , and L. G. Tateosian³

¹Department of Civil, Construction, and Environmental Engineering, North Carolina State University, Raleigh, NC, USA,

²Department of Civil, Construction, and Environmental Engineering, University of Delaware, Newark, DE, USA, ³Center for Geospatial Analytics, North Carolina State University, Raleigh, NC, USA

Abstract Storm tides—the combination of tides and storm surge—cause flooding in coastal regions, often with differences in magnitudes between the open coast and locations within water bodies like bays and estuaries. Previous studies have shown that storm surge is sensitive to the storm's wind intensity, speed, and track; the coast's geometry and relative position to the storm; and also to nonlinear interactions with tides. These sensitivities have been documented at either open coast or bay locations, but without comparing or quantifying the differences in behavior between them, even though these differences may have implications for risk management. This study examines the range of peak storm tides within the Lower Chesapeake Bay, which has vulnerable communities at the open coast, like Virginia Beach, and inside the bay near the James River, like Hampton and Norfolk. A high-resolution model was developed for the region and validated against observations of water levels during Hurricane Irene in 2011. Storm parameters were perturbed to analyze the variation in storm tide ranges. It was found that the range of possible storm tides was greater at bay locations than at the open coast, by as much as 47%. This higher variability at the bay locations was due to sensitivities to storm parameters like the wind intensity and storm tracks, which led to storm tide peaks outside of the interquartile range. This finding highlights the importance of understanding the uncertainty in storm forecasts concerning future possible impacts in complex coastal regions.

Plain Language Summary Hurricanes and other storms can push water to the coast and cause flooding. This elevated water, known as storm surge, can be more or less severe, depending on the strength and movement of the storm, on the shape of the coast, and on whether the storm surge arrives with the normal high tide. The hazard may be harder to predict at locations inland from the coast, where these factors may combine to increase the range of possible flood levels. This study examines how storm surge and tides may vary in the Lower Chesapeake Bay, a region that floods often. A computer model was used to predict the storm surge and tides during Hurricane Irene in 2011, and then we varied that storm's strength and movement to explore how different storms may affect the region. We compared the predictions of water levels at locations on the open coast and within the bay, and we saw that the range of peak water levels is larger inside the bay.

1. Introduction

Flood risks due to storm tides can be different along open coasts compared to bays. Tides and storm surge, defined as the storm-induced increase in water levels (National Oceanic and Atmospheric Administration, 2024a, 2024b), can combine as *storm tides* to cause flooding that varies in coastal regions. Storm tides at the open coast can reach extreme magnitudes, such as the peaks of 8.8 m along the Mississippi coast during Katrina in 2005, 6.1 m along the Texas coast during Ike in 2008, 4.6 m along the New Jersey coast during Sandy in 2012, and up to 4.6 m along the Southwest Florida coast during Ian in 2022 (National Weather Service, 2025a; National Weather Service, 2025b; U.S. Geological Survey, 2016; Bucci et al., 2023). However, storm tides are often larger in bays, channels, and rivers (M. Li et al., 2006). Between open-coast and bay locations, the differences in storm tides can be as much as 0.5–1.0 m (Stark et al., 2015; Thomas et al., 2019).

Storm tides are more complex inside bays. The relatively shallow bathymetry allows for bay waters to respond quickly to a storm (Islam et al., 2021), depending on how the storm's track aligns with the bay (Qian et al., 2024). Strong winds can draw down the water in the bay, for example, the drying of parts of Pamlico Sound during Irene in 2011 (Bowers, 2012) or Tampa Bay during Ian in 2022 (Bucci et al., 2023). As Ike approached Texas in 2008, waters were drawn away from the Galveston Bay's northeast side, where the storm tides were smaller than the

© 2025. The Author(s).

This is an open access article under the terms of the [Creative Commons Attribution-NonCommercial-NoDerivs License](https://creativecommons.org/licenses/by/4.0/), which permits use and distribution in any medium, provided the original work is properly cited, the use is non-commercial and no modifications or adaptations are made.

Validation: Jenero S. Knowles, J. C. Dietrich, A. E. Elkut, J. A. Puleo, F. Shi
Visualization: Jenero S. Knowles, J. C. Dietrich, A. E. Elkut, J. A. Puleo, F. Shi, L. G. Tateosian
Writing – original draft: Jenero S. Knowles, J. C. Dietrich
Writing – review & editing: Jenero S. Knowles, J. C. Dietrich, A. E. Elkut, J. A. Puleo, F. Shi, L. G. Tateosian

devastating floods at Galveston and Bolivar Peninsula at landfall (A. G. Sebastian et al., 2014). Thus, a bay may have a *range of peak storm tides* that is larger than at the open coast. This range may vary across storms. For example, differences can be seen in the storm tides at the same locations during two recent storms: Nicholas, which was a slow-moving, short-lived Category 1 storm in 2021, and Beryl, which was a longer-lasting Category 5 storm in 2024. At locations near the open coast (National Oceanic and Atmospheric Administration, 2024a, 2024b), their peak storm tides were similar, for example, at the entrance to Galveston Bay, the maxima were 1.22 m during Nicholas and 1.32 m during Beryl (difference of 0.10 m). But farther inland, their maximum storm tides were different; for example, at Morgan's Point closer to Houston, the maxima were 1.62 m during Nicholas and 1.87 m during Beryl (difference of 0.25 m).

There is a need to quantify how the range of peak storm tides may vary between open coasts and bays and how the range may be sensitive to specific storm parameters. Predictions of storm tides are essential for rapid response and long-term planning (Khalid et al., 2021). At least for Nicholas and Beryl, emergency management and planning (Sadri et al., 2015; Yang et al., 2019) may be similar near Galveston (at the open coast) but different closer to Houston (up the bay). In general, predictions may be more challenging for bay locations with larger variability in the hazard.

Previous studies have examined the sensitivity of storm tides to the storm characteristics and/or coast configuration, but not with a focus on the range of peak storm tides in bays relative to the open coast. Several studies have focused on storm characteristics (e.g., Salisbury & Hagen, 2007; Rego & Li, 2010; F. Zhang & Li, 2019; Z. Zhang et al., 2022; Shashank et al., 2024). An increase in wind intensity can increase the storm surge (Shashank et al., 2021), and this effect can be magnified when coupled with forward speed (Musinguzi et al., 2021). Storms with a larger radius of maximum winds can also produce larger storm surges in specific regions (Irish et al., 2008; J. Li et al., 2019). Slower storms can increase flooding by allowing more time for surges to travel farther inland, while faster storms can create higher peak surges near the coast (Park & Youn, 2021; Rego & Li, 2009), although this finding may not be generalizable to all coasts (Weisburg & Zheng, 2006). Storms with approach angles less than 90° to the coastline may generate Kelvin waves, which can also affect the total water levels (Pandey & Rao, 2019; M. Sebastian et al., 2019). Other studies have focused on estuaries and bays. The maximum storm tide in a bay occurs when maximum winds are at the mouth of the bay, as seen in Tampa Bay (Weisburg & Zheng, 2006). For Galveston Bay, different locations may respond to storm tides depending on the coastal geometry (Bass et al., 2018). The magnitudes were generally smaller along the coast compared to locations inside the bay, except when the storm was east of the bay with dominant offshore winds. The position of the storm track relative to a bay can affect the magnitudes of storm tides (Du et al., 2020; Ramos-Valle et al., 2020). While these studies inform how storm tides respond to storm characteristics and/or in a bay, they neither quantify the range of peak storm tides relative to the open coast, nor identify the factors to cause differences between these locations.

In this study, we investigate variability in peak storm tides at open-coast and bay locations. *We hypothesize that the range of peak storm tides will be larger at bay locations farther from the coast, primarily due to variations in storm intensity and position, in combination with local geographic conditions.* We emphasize that our focus is on the range of storm tides, that is, the difference between the maximum and minimum of the peak storm tides. The overall peaks for some storms may be larger at the open coast, but we expect the storm-to-storm range in peaks to be larger at bay locations. This study uses the ADvanced CIRCulation (ADCIRC) model (Luettich & Westerink, 2004; Westerink et al., 2008) to quantify the storm tides and their ranges at locations near and inside Chesapeake Bay, which is the largest estuary in the United States (Chesapeake Bay Foundation, 2024) and has seen an increase in storm frequency over the past centuries (National Weather Service, 2022). Storm variability will be included via perturbed scenarios of Irene in 2011, and geographic variability will be assessed at three locations from the open coast to inside the bay. The primary objectives are to quantify the range in the peak storm tides at various locations in Chesapeake Bay and to identify the primary factors that drive this variability.

2. Methods

2.1. Study Site

Chesapeake Bay is located in the Mid-Atlantic region of the United States (Figure 1). We focus on the lower part of the bay, where there are dynamic interactions between tides entering the bay's mouth and potential flooding of the Virginia communities of Norfolk, Hampton, and Virginia Beach (VAB). In this region, tides and currents are stronger and more consistent compared to the middle and upper sections of the bay (Hallock et al., 2003; Shi

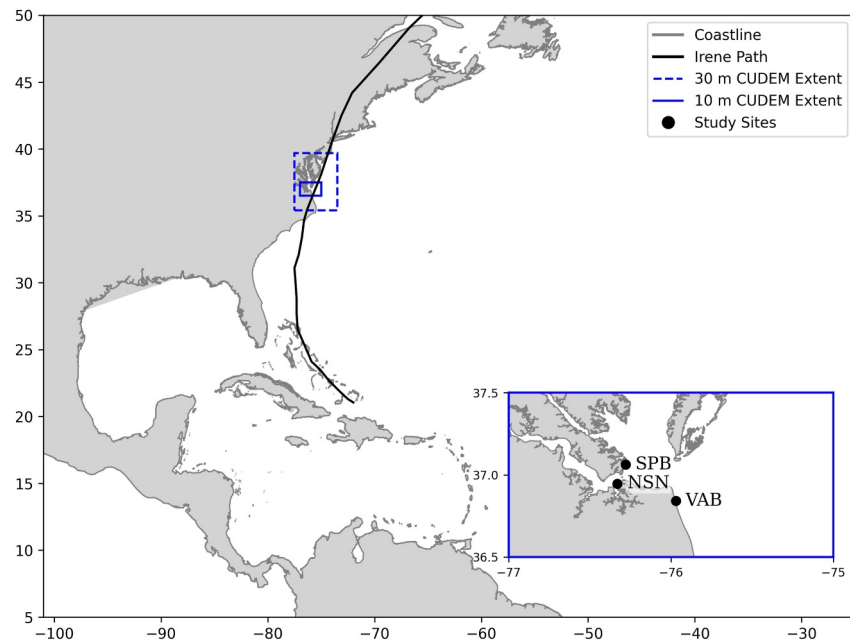


Figure 1. Path of Irene and spatial extents of the digital elevation models (DEMs) used to analyze variations in peak storm tides. The Shuttle Radar Topography Mission (SRTM) DEM covers the entire area of the main map, while the dashed line shows the coverage of the 30-m Continuously Updated DEM (CUDEM), and the inset shows the coverage of the 10-m CUDEM. The NHC best track for Irene is overlaid, marking its path relative to study sites: Naval Station Norfolk (NSN), Salt Pond Beach (SPB), and Virginia Beach (VAB).

et al., 2013) due to frequent river discharges and the influence of oscillations from the Gulf Stream (Ezer et al., 2022). During storm events, water levels can rise dramatically due to the funneling effect of the bay, with tides amplified by wind-driven surges (Lee et al., 2017). The bay's water levels were affected by storms including Isabel in 2003, Irene in 2011, Sandy in 2012, Michael in 2018, and Dorian in 2019, even though these storms tracked offshore of Chesapeake Bay and had their worst effects elsewhere. The region remains vulnerable to storm surges and coastal flooding due to its low elevation and location along the U.S. Atlantic coast.

The region is described by geospatial data sets for ground surface elevations as digital elevation models (DEMs), as well as for land cover and land use. For the northwest Atlantic Ocean, the 2018 Shuttle Radar Topography Mission (SRTM; U.S. Geological Survey, 2018) has a minimum resolution of 500 m between (101° W, 5° N) to (25° W, 50° N). For the Mid-Atlantic, the 2014 Continuously Updated DEM (CUDEM; Amante et al., 2023) includes the states of Virginia, Maryland, and Delaware with a minimum resolution at 30 m between (77.55° W, 35.4° N) to (73.5° W, 39.7° N) after resampling and clipping the 1/3 arc-second CUDEM for this region. The Lower Chesapeake DEM, which is a higher-resolution version of the CUDEM, spans the southern part of the Chesapeake Bay where VAB, Norfolk, and Hampton meet the Atlantic Ocean with a minimum resolution at 10 m between (76.57° W, 36.77° N) to (75.75° W, 37.18° N) after resampling and clipping the 1/9 arc-s CUDEM for this region. The extents of these DEMs are shown in Figure 1 over the full domain of the SRTM. These DEMs were clipped to the region of interest and resampled for use in mesh generation. In addition, features like marshes, forests, developments, and water bodies are represented via data about land cover and land use. The 2016 Coastal Change Analysis Program (CCAP) Regional Land Cover and Change data set covers the Mid-Atlantic region and includes 24 classifications of land use and land cover for wind reduction factors and canopy coefficients at a 30-m resolution (National Oceanic and Atmospheric Administration, Office for Coastal Management, 2016).

In this study, storm tides were simulated through the region with a focus at three locations: VAB, Salt Pond Beach (SPB), and Naval Station Norfolk (NSN). These locations progress from the open coast (VAB) into open (SPB) and protected (NSN) sites in the bay (Figure 1). At VAB, we analyzed at its boardwalk and public beach (75.97° W, 36.84° N), which are located at the open coast and should see the full effects of storm tides. At SPB, we analyzed at a fishing pier (76.28° W, 37.06° N) near a beach in Hampton, which is located within the bay but is

open to the bay's mouth. At NSN, we analyzed at the NOAA long-term tide gauge at Sewells Point, located on the east side of Norfolk near the largest naval station in the world (Marley, 2017).

2.2. Storm Tide Model

2.2.1. ADCIRC

We used the ADCIRC (Luettich et al., 1992; Westerink et al., 2008) model to represent the effects of tides and storm surge in south Chesapeake Bay. ADCIRC has been used successfully in Chesapeake Bay to investigate the uncertainties of model choices for large estuaries (Garzon & Ferreira, 2016) and also for an extensive storm surge analysis for the Mid-Atlantic region (Blanton et al., 2011). ADCIRC is recognized widely for storm surge forecasts (Coastal Emergency Risks Assessment, 2024), historical storm analyses (Bilskie & Luettich, 2024; Danso & Patricola, 2024), assessment and design of protective infrastructure (Fahad & Nazari, 2021; Sichani et al., 2020), and the creation of flood risk maps (FEMA, 2021). ADCIRC uses the continuous-Galerkin, finite element method to solve modified forms of the shallow water equations on unstructured meshes (Luettich & Westerink, 2004).

For the ADCIRC simulations, the tides were forced by using information from the TPXO global model for the barotropic tide database (Egbert & Erofeeva, 2002) using the major 8 tidal constituents (K_1 , O_1 , Q_1 , P_1 , M_2 , N_2 , K_2 , and S_2). The two-dimensional, depth-integrated, explicit solver was used at 1-s time intervals to solve the lumped generalized wave continuity equation (Kinnmark, 1986). For this study, we developed a mesh with the highest spatial resolution in the south Chesapeake Bay (Section 2.2.2). The eddy viscosity was specified with a constant value of 50 m²/s. Wetting and drying were enabled, with a minimum water depth of 0.1 m and a minimum velocity for wetting of 0.01 m/s. Advective terms were disabled to simplify and stabilize the simulation.

2.2.2. Unstructured Mesh

A high-resolution, unstructured, finite element mesh was developed using OceanMesh2D (Roberts et al., 2019). This mesh covers the northwest Atlantic Ocean basin, extending to just west of the 50° longitudinal connecting Nova Scotia, Canada, to Paramaribo, Suriname, but with the highest spatial resolution in the Lower Chesapeake Bay (Figure 2). Inside the extents of this mesh, a tropical cyclone can be initialized in the open ocean, and then its effects can be simulated on the continental shelf and into the coastal region. The mesh has about 2.54 million elements and 1.26 million vertices.

The spatial resolution varies across the domain from the Lower Chesapeake Bay into the Atlantic Ocean, using three stages with minimum resolutions of 20 m at the opening of the bay, 60 m in the Mid-Atlantic region, and 1 km in the Atlantic Ocean. Near the ocean boundary, the resolution ranges between 10 and 30 km. For the entire mesh, the resolution was controlled from the coastlines and coarsened outward to the limits of each DEM by requiring each element to be no more than 20% larger than its neighbors. Ground surface elevations were assigned to the mesh vertices via interpolation from the DEMs, with preference for the finest-resolution DEM near Norfolk, Virginia. The mesh transitions to a coarser resolution farther from the study locations to optimize computational efficiency. Nodal attributes, which are constant in time but vary spatially, were also developed at the mesh vertices by using information from CCAP data (Westerink et al., 2008). These nodal attributes include Manning's n , surface directional effective roughness length, canopy coefficient, and the primitive weighting factor τ_0 . The land cover data sets were converted to Mannings's n values (Owensby et al., 2020) in the Mid-Atlantic region, and a constant $n = 0.02$ was applied in open water. The surface directional effective roughness length and canopy coefficients were also derived from the CCAP data sets and were interpolated onto the mesh using the ADCIRC Module toolkit (Cobell, 2020). For τ_0 , the values were applied using utilities in OceanMesh2D in two classes with values of: 0.005 if the node had a depth greater than 10 m or was more than 2 km away from the coastline, and 0.03 elsewhere.

2.3. Storm Simulations

2.3.1. Irene

Irene began as a tropical wave that left the African coast on 15 August 2011. As the tropical wave approached the Lesser Antilles on 20 August, it became a tropical depression and then a strong tropical storm as it made its first landfall in Puerto Rico. The other three landfalls included North Carolina, New Jersey, and New York, with the

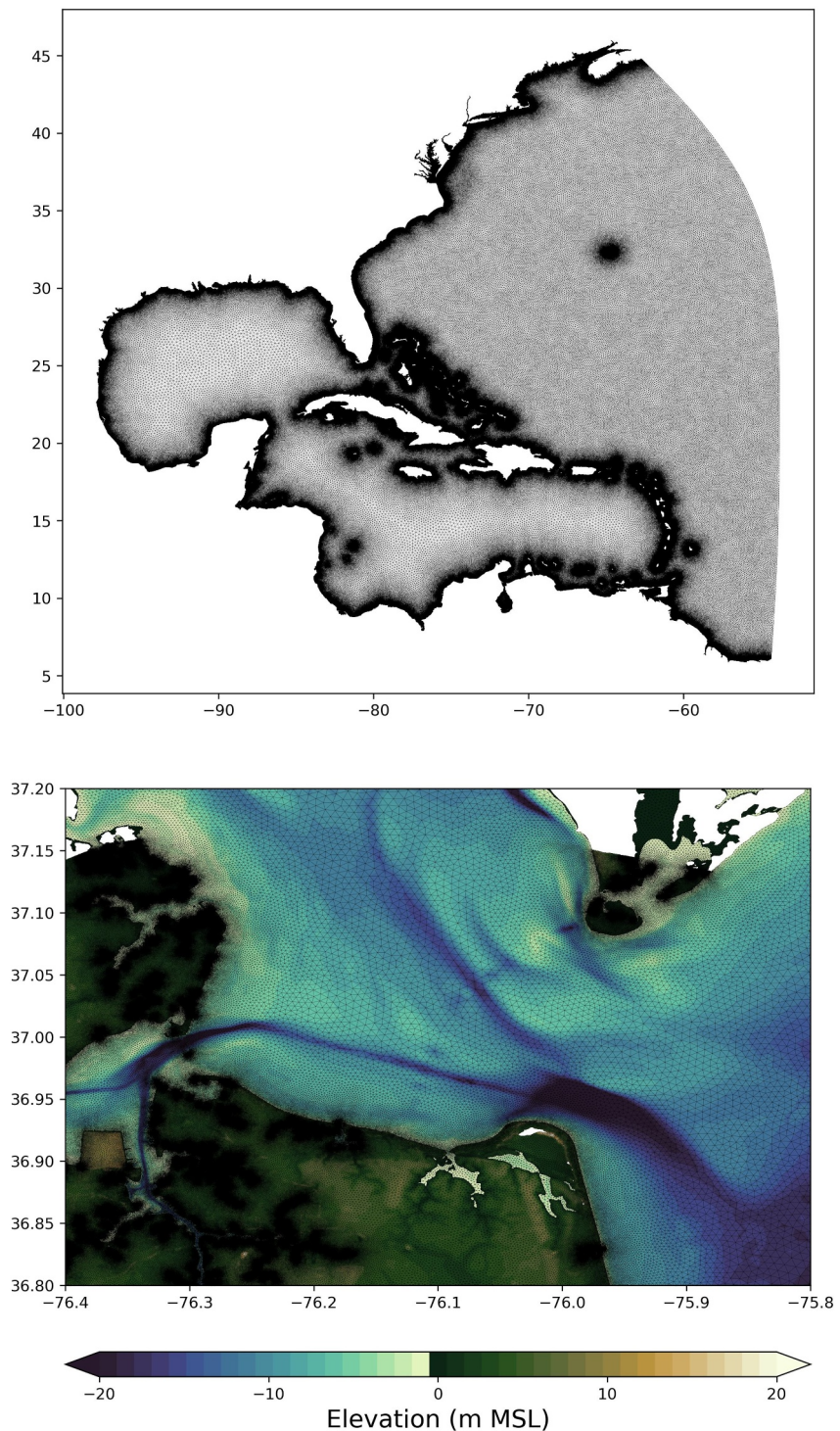


Figure 2. A high-resolution computational mesh was developed to assess storm tides in the Lower Chesapeake Bay Region: (top) full domain of the mesh into the Atlantic Ocean; and (bottom) highest resolution at the Lower Chesapeake Bay, where the mesh resolution increases to 20 m.

landfall in North Carolina being the only hurricane landfall (Avila & Cangialosi, 2013). After Irene passed over North Carolina, it moved just east of the opening of the Chesapeake Bay. Irene reached a peak wind intensity of 51 m/s, Category 3 on the Saffir-Simpson scale, on 24 August as the storm moved over the Bahamas. However, at its landfall near Cape Fear, North Carolina, Irene sustained hurricane-force winds to the Outer Banks and

hurricane-force gusts over Northern Virginia and the Chesapeake Bay (National Oceanic and Atmospheric Administration, 2011). Over the next few days, Irene weakened to a tropical storm heading north where gusts ranged from 27 to 31 m/s in New York City. At Sewells Point, a NOAA observation station in the south Chesapeake Bay, tides ranged between -0.20 and 0.52 m before the storm. During the storm, water levels rose above the predicted tide range for 36 hr. The peak storm tide was 1.89 m, coinciding with a high tide at this location.

Water levels were elevated in the Lower Chesapeake Bay, even before the arrival of Irene. This increase in the mean water levels was likely caused by a combination of antecedent atmospheric forcings, river runoff, and longer-term oceanographic processes (Kerns & Chen, 2023; Little et al., 2019), none of which are represented in our storm simulations with ADCIRC. Thus, to account for these processes, a vertical offset was computed by averaging the observed tides at Sewells Point for the 7.2 days (14 tidal cycles) before the storm from 0000 UTC 06 August to 0000 UTC 24 Aug. During that period, the observed mean water level was computed as 0.127 m (MSL), which we applied as an initial vertical offset in the water levels in our simulations.

Surface pressure and wind fields were simulated with the Generalized Asymmetric Holland Model (GAHM; Gao, 2018; Dietrich et al., 2018), which was a modified version of the parametric model from Holland (1980). GAHM can predict a different profile in each storm quadrant, does not assume a cyclostrophic balance, and can match both the wind speed, $V = V_{\max}$, and its gradient, $dV/dr = 0$, at the radius to maximum winds, $r = R_{\max}$. GAHM was implemented within ADCIRC to accept a few storm parameters (e.g., from the NHC best-track files in ATCF format, National Hurricane Center, 2011) and then develop the atmospheric forcing at every mesh vertex. GAHM's predictions of surface pressures and winds may not be as accurate as those from a full-physics deterministic model (Dietrich et al., 2018), but its adaptability to changing storm parameters will allow for perturbed scenarios of Irene in this study.

Simulations were run in two stages. First, a spin-up simulation was completed for 18 days starting at 0000 UTC 6 Aug. Tides were ramped during the first 12 days and then continued for an additional 6 days to achieve a dynamic equilibrium before atmospheric forcings were applied. Then, a storm simulation was completed for Irene for 6 days from 0000 UTC 24 August to 0000 30 Aug. The exception was the simulation (described below) analyzing the forward speeds of the storm in which the storm duration was different than 6 days. For those simulations, the 18-day spin-up was chosen before the storm to allow the peak storm tides to occur near 0000 UTC 28 Aug, similar to Irene.

2.3.2. Perturbations to Irene

The relationship between storm parameters and storm-tide response was explored via perturbations to Irene. Small changes in the position of Irene could have resulted in worse conditions (Ezer, 2019; Hoffman & Gombos, 2012). Although other storms could have been analyzed, the objective is to determine how the range of possible storm tides differs at the coast and bay locations. With its known effects and its potential for worse conditions, Irene was the best-suited storm to perturb and analyze for this region. We used a systematic approach to represent a variety of storms that could potentially impact the Lower Chesapeake Bay. By using a variety of perturbations to a single storm, we expect that there would be a range of storm tides produced from the changes in storm parameters. This range would then be further analyzed against our hypothesis.

The base simulation was perturbed by altering the wind intensity, radius of maximum winds, forward speed, angle of approach, and storm track (Table 1). The wind intensity was modified following the studies of Camelo et al. (2020) and Emmanuel (1987) in which the peak wind speed can increase by 5% for every degree of sea surface temperature increase. We modified the wind speeds by -7.5% , $+7.5\%$, and $+22.5\%$, corresponding to potential sea surface temperature increases of -1.5° , $+1.5^\circ$, and $+4.5^\circ$. The radius of maximum winds was modified following the study of Mousavi et al. (2011), which perturbed the radius by -10% , $+10\%$, and $+25\%$. These perturbations led to significant changes in the wind magnitudes.

The forward speed was modified using factors of 0.5, 1.0, 1.5, and 2.0 times the storm's speed following the changes by Thomas et al. (2019) and Qian et al. (2024). This was accomplished by varying the time between the increments in the NHC best track, and thus factors larger than unity will correspond to a faster storm (with less time between snaps). The angle of approach was perturbed by rotating the storm at the point where the eye is on the coast at the state border between North Carolina and Virginia at the reference point (75.84° W, 36.45° N). The

Table 1
Summary of Perturbations Applied to Irene From the Base Storm Simulation

Parameter	← Weak/Slow/West			Base	Strong/Fast/East →		
Wind speed				1.0	1.075		1.225
Storm size				1.0	1.1		1.25
Storm speed				1.0	1.5		2.0
Track shift (km)	-255	-178	-100	0	100	178	255
Track rotation (°)				0	15	45	75

Note. Perturbations to wind speed and storm size were applied as factors multiplied by the maximum wind speeds and radii to maximum winds, respectively, with positive factors as an increase. Perturbations to storm speed were applied as factors multiplied by the 6-hr increment between the time snaps, with positive factors as a speed-up. Perturbations to shift the storm track were applied as offsets in longitude, with positive offsets as a shift eastward. Perturbations to rotate the storm track were applied as rotation angles, with positive angles as a counterclockwise rotation.

storm was rotated counterclockwise for -15° , 15° , 45° , and 75° , so the most-intense winds and storm surge can impact the Chesapeake Bay (Pandey & Rao, 2019). Following the storm track changes from Salehi (2018), we shifted the storm track by adjusting the longitudes in multiples of the radius of maximum winds at 100 km (55 nm) on either side of the base track (Figure 3).

2.4. Analysis Metrics

We developed tools to consider the perturbed storms' effects on the ADCIRC predictions of storm tides throughout the region. Time series were extracted from the predicted water levels at NSN, SPB, and VAB between 25 August 2011 and 29 August 2011 to show the variation of storm tides. This time series allowed us to determine the peak water levels and perform calculations for the correlation coefficient (R):

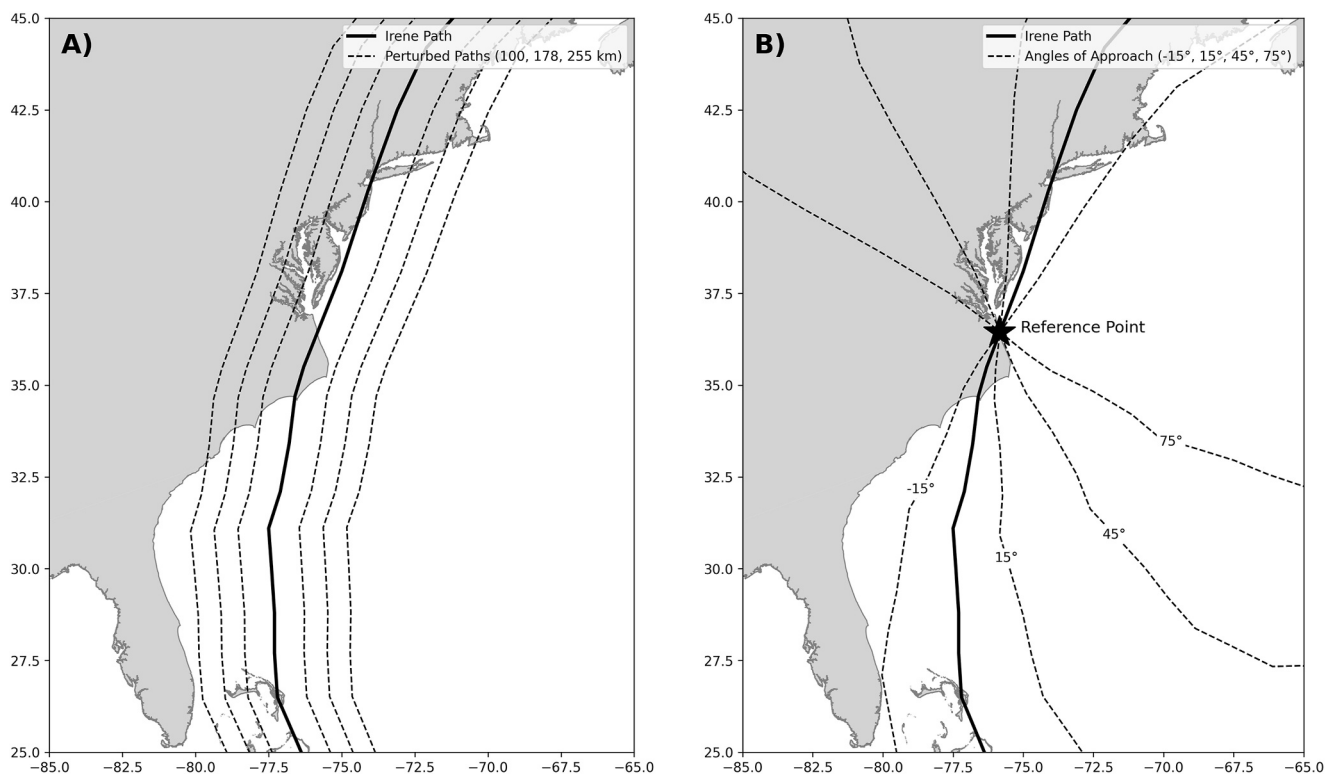


Figure 3. Perturbations to Irene's path based on NHC best track data, highlighting potential storm trajectories affected by (a) position and (b) angle of approach. Panel A illustrates Irene's path with eastward and westward shifts (dashed lines) at intervals of 100, 178, and 255 km. Panel B depicts rotated trajectory variations (dashed lines) at angles of -15° , 15° , 45° , and 75° relative to the location (75.84° W, 36.45° N) where Irene reentered the Atlantic.

$$R = \frac{\sum_{i=1}^N (x_i - \bar{x})(y_i - \bar{y})}{\sqrt{\sum_{i=1}^N (x_i - \bar{x})^2 \sum_{i=1}^N (y_i - \bar{y})^2}}, \quad (1)$$

and the root-mean-square error (RMSE):

$$\text{RMSE} = \sqrt{\frac{1}{N} \sum_{i=1}^N (x_i - y_i)^2}, \quad (2)$$

in which N represents the number of observed and predicted data points, x_i represents the observed values from the NOAA Station 8638610 at Sewells Point, and y_i denotes the predicted values from the ADCIRC model. The terms \bar{x} and \bar{y} are the time-averaged means of the observed and predicted values, respectively. The terms $(x_i - \bar{x})$ and $(y_i - \bar{y})$ represent the deviations of individual observed and modeled values from their respective means and are used to compute variance and covariance. The residuals $(x_i - y_i)$ measure the differences between the observed and modeled values, serving as the basis for calculating errors like RMSE.

These variables quantify the relationship and the degree of agreement between the observed and modeled data. The correlation coefficient describes how the modeled and observed time series are correlated to each other. A value close to unity shows a direct relationship between the observation data and the predicted results, strengthening the model's validity. Generally, a value greater than 0.8 is considered a strong correlation and is accepted within the field (U.S. Army Corps of Engineers, 2013). The RMSE was used to determine the difference between the predicted values and the observed values. It is also used to evaluate the model's accuracy in making predictions. An RMSE between 0.1 and 0.2 m is good for detailed hindcasts, while values less than 0.3 m are acceptable for operational forecasts (Kerr et al., 2013).

3. Results

3.1. Storm Tides in the Lower Chesapeake Due To Irene

The ADCIRC predictions have an acceptable accuracy. At NSN, the storm tides from the base simulation of Irene had an RMSE = 0.203 m and an $R = 0.956$, which are similar to error metrics in previous ADCIRC hindcasts (Azad & Marsooli, 2024; Dietrich et al., 2011). The difference in peak storm tides was 0.31 m, which is slightly higher than that found in typical ADCIRC hindcasts (Bilskie & Luettich, 2024; Hope et al., 2013), and errors may be due to our use of GAHM instead of a full-physics atmospheric model. It has been shown (Cyriac et al., 2018; Dietrich et al., 2018) that the use of atmospheric forcing from parametric models (like GAHM) can lead to less accurate predictions of storm surges. However, in this study, GAHM is beneficial because it allows for perturbation of individual storm parameters, and thus a thorough examination of the factors that contribute to variability in the peak storm tides.

As Irene approached the bay's entrance, its winds blew westward from the Atlantic Ocean, but as the storm progressed, its winds shifted eastward. These changing winds had different effects on the ADCIRC predictions of maximum storm tides. At the open coast, the maximum storm tides ranged from 1.72 m at VAB to 2.05 m north of the bay's opening (Figure 4). Within the bay, the maximum storm tides ranged from 1.99 m in the north to 2.12 m in the south near SPB, reflecting the north-to-south alignment of Irene's winds with the bay's major axis. Closer to the James River near NSN, the maximum storm tides ranged from 2.15 to 2.25 m, due to the narrowing of channels with consistent water depths.

At NSN, the maximum storm surge occurred within 1 hour of the high tide observed at Sewells Point. Peak storm tides occurred earlier at VAB on the open coast, but they increased at SPB and NSN for a longer duration, when using a water level of 1 m as a flood threshold. The predicted peak storm tides were 2.20 m at NSN, 2.03 m at SPB, and 1.72 m at VAB. After Irene passed and wind directions reversed, a larger negative storm tide (drawdown) was predicted at coastal sites than inland sites, with water levels as low as -0.97 m at VAB (e.g., blue line in Figure 5c).

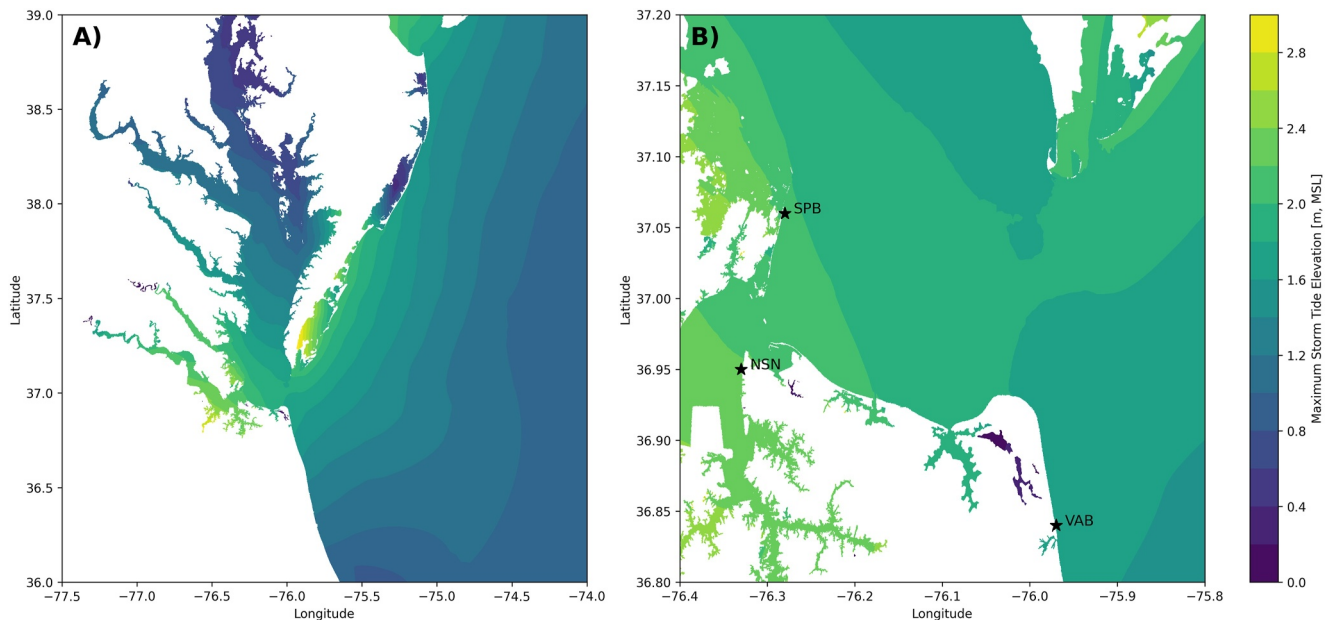


Figure 4. The ADCIRC-predicted maximum storm tide elevations in (a) the U.S. Mid-Atlantic coast and (b) the Lower Chesapeake Bay.

3.2. Variations in Ranges of Peak Storm Tides

During Irene, the peak storm tides were predicted to be higher inside the bay (e.g., 2.20 m at NSN; blue line in Figure 5a) than at the open coast (e.g., 1.72 m at VAB; blue line in Figure 5c). However, we are interested in how the storm tides vary across many possible storms (e.g., gray lines in Figure 5), and especially how the range of peak storm tides may vary spatially. Several trends are evident in the time series. Most of the perturbed storms do not affect the water levels until about 12 hr before the peak, except for one storm, a slowed down Irene at a factor of 0.5, that causes an increase in water levels for multiple days beforehand. At the peak, there is significant variability in the water levels across the storms, with the base Irene simulation near the median. The overall peak storm tides do increase from the open coast to the bay locations. Some storms cause a drawdown in the 12 hr after the peak, but other storms continue to elevate the water levels above the base simulation. In this section, we examine the range of peak storm tides, which we compute as the difference between the maximum and minimum of the peak water levels as predicted by ADCIRC for simulations of Irene and its perturbations.

At every location that is always wet during Irene and its perturbations, the range of peak storm tides was computed (Figure 6). The ranges in peak storm tides are about 1 m at the open coast and the opening of Chesapeake Bay, but the ranges increase to 2 m or higher in the western bay and into the James River. The range was affected by different storms, that is, the storm corresponding to the maximum of maximum at the open coast was different than the storm corresponding to the same value inside the bay. The storms with stronger wind intensities showed the highest maximum storm tides at NSN and SPB because their strongest winds aligned with the major axis of the Chesapeake Bay and pushed water toward Hampton and Norfolk. The storm with the angle of approach closest to shore-perpendicular had the highest maximum storm tide at VAB because its track facilitated water transport toward VAB. The same effect was seen for the minimum of maximum, where different storms corresponded to the values contributing to the overall range. The eastward shift of the storm track showed the lowest maximum storm tides at NSN and SPB, while the westward shift had this effect at VAB.

These trends can be quantified at the analysis locations, at which the ranges in peak storm tides were affected differently by the storm scenarios (Figure 7). Some perturbations caused a significant increase in the range from the open coast to the bay locations:

- *Wind intensity*: Stronger winds exacerbated the trends during Irene, with more water pushed into the Lower Chesapeake Bay. Across these scenarios, the range of peak storm tides was 0.48 m at VAB, 0.86 m at SPB, and 1.05 m at NSN.

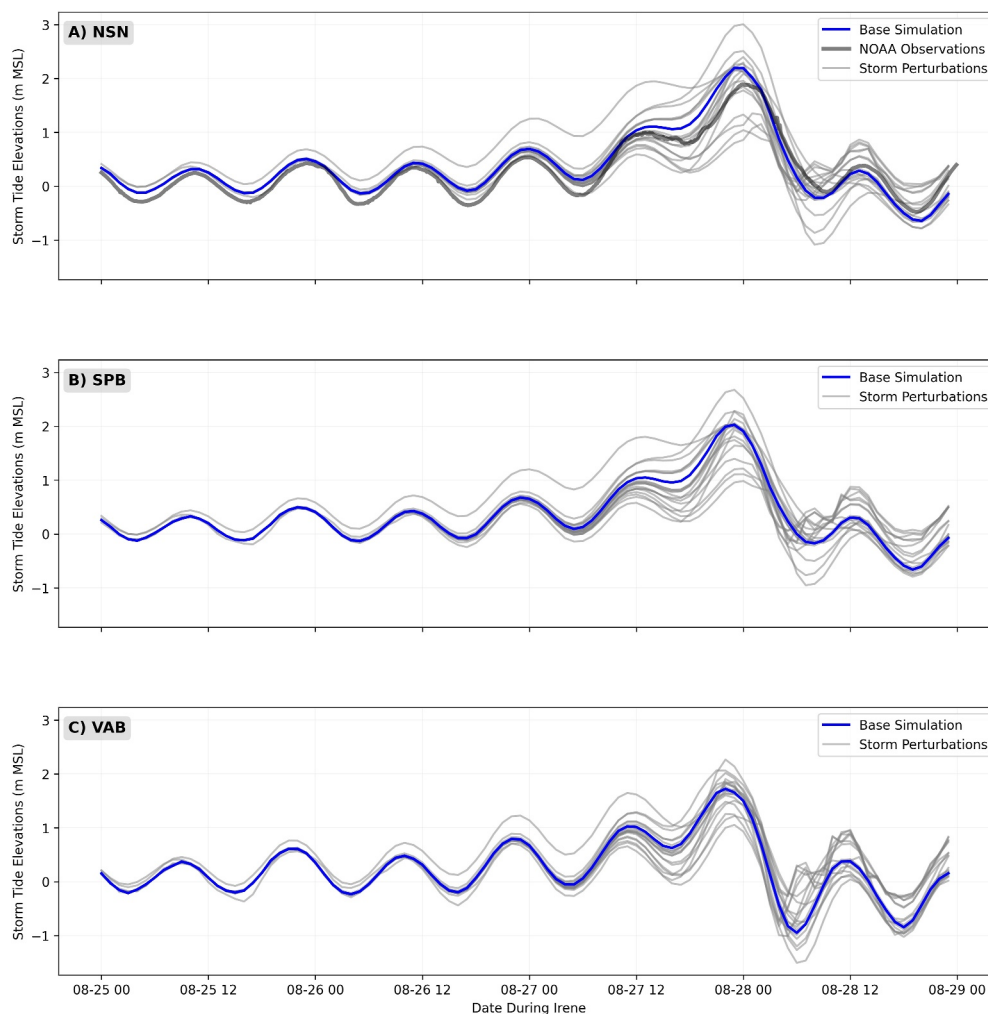


Figure 5. Variability of storm tides during Irene at (a) Naval Station Norfolk (NSN), (b) Salt Pond Beach (SPB), and (c) Virginia Beach (VAB). The base simulation (blue line) shows a prediction for Irene. The storm perturbations (light gray lines) show the time series from perturbations to the wind intensity, storm size, forward speed, storm track, and approach angle. At NSN, the observations (dark gray dots) from Sewells Point are shown.

- *Track shift:* When the storm was shifted away from the region, the peak storm tides decreased, although the ranges were influenced significantly by the alignment of the wind fields with the Chesapeake Bay. Across the eastward shifts, the range of peak storm tides was 0.50 m at VAB, 1.05 m at SPB, and 1.16 m at NSN, whereas across the westward shifts, the range of peak storm tides was 0.67 m at VAB, 0.92 m at SPB, and 1.04 m at NSN.

However, for other perturbations, the range of peak storm tides did not show a significant trend from the open coast to inside the bay:

- *Storm size:* Little to no impact was observed on the storm tide elevations throughout the bay. The most variation in storm tide elevation size was seen along the coast, while the bay locations remained consistent. The range of peak storm tides was 0.12 m at VAB, 0.02 m at SPB, and 0.03 m at NSN.
- *Forward speed:* Little to no impact was observed on the storm tide elevations throughout the region. However, the exception was at the coast. The range of peak storm tides was 0.19 m at VAB, 0.07 m at SPB, and 0.07 m at NSN.
- *Approach angle:* The approach angle greatly influenced the range of storm tides in the region. However, a counterpositive result was observed as ranges decreased further at the bay locations. The range of peak storm tides was 0.64 m at VAB, 0.23 m at SPB, and 0.19 m at NSN.

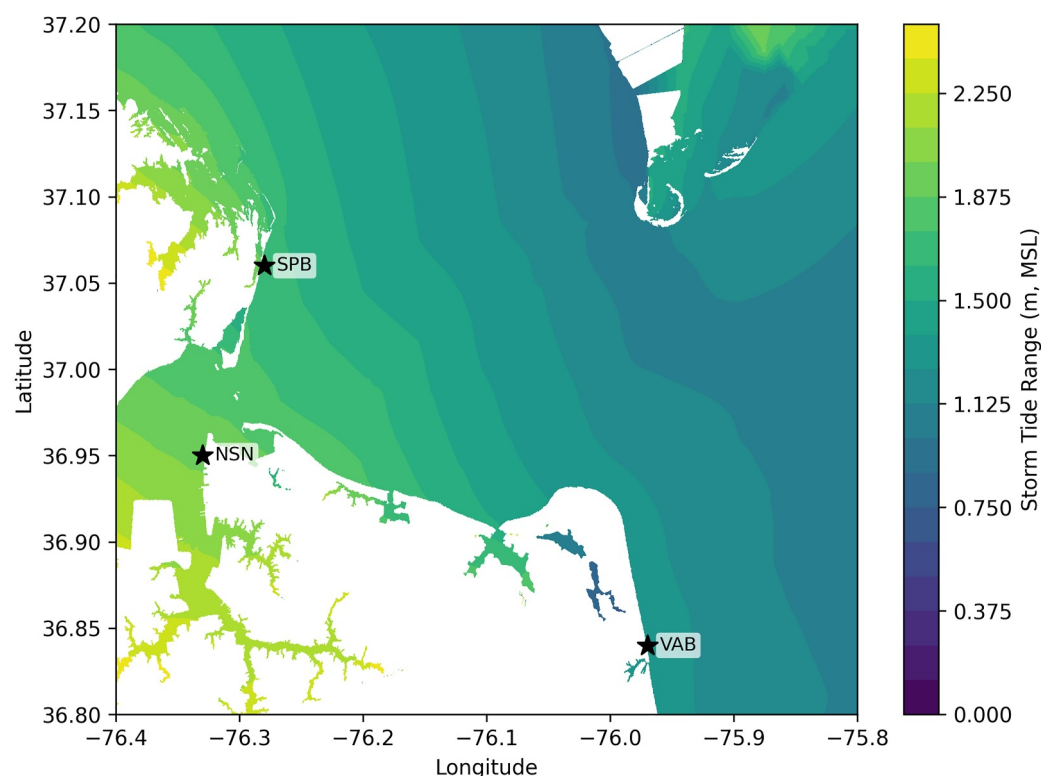


Figure 6. Range of maximum storm tides at all locations within the Chesapeake Bay for all storm simulations. The plot highlights the spatial variability of peak storm tides across the bay.

Overall, we observe that the position of the storm and wind intensity were the driving factors in the range of peak storm tides. Table 2 summarizes the values for the ranges of peak storm tides at NSN, SPB, and VAB from the perturbations of the storm parameters.

At these locations, we consider the overall range of peak storm tides for Irene and all perturbations (Figure 7). The range of peak storm tides is smallest at the open coast (VAB, 1.22 m), and it increases inside the bay (SPB, 1.70 m; NSN, 1.97 m). While the storm tides for the base simulations are higher, the interquartile range (IQR) also validates our hypothesis, showing the IQR is larger for the bay locations than at the open coast. The IQRs are 0.28 m (VAB), 0.33 m (SPB), and 0.40 m (NSN). A few trends were observed from the results at all locations. An increase in wind intensity increased storm tide elevations. This rate of increase was seen more at the bay locations than at the coast. Wind intensity and angles of approach were the major drivers for the upper limit of the storm tide ranges, being above the IQR. The storm tide elevations from the storm size were very similar at the bay locations. However, small changes were seen on the coast. Shifts in the storm track also influence the range of storm tides within the bay. At all study sites, the storm tide elevations were reduced by shifting the storm tracks. In addition, these elevations fell below the IQR. Because the wind intensity, storm tracks, and approach angles were outside of the IQR, proving to influence the range of storm tide elevations, these parameters were considered the most influential to the range of storm tides at the coast and bay locations.

4. Discussion

Previous studies have assessed the influence of individual storm parameters on storm tides (e.g., Fossel et al., 2017; Musinguzi et al., 2021). However, those studies did not compare the ranges of peak storm tides at the open coast and bay locations. Via simulations with base and perturbed scenarios of Irene, we showed that the range of peak storm tides is larger, by at least 47%, in the bay than at the open coast. The peak is not necessarily higher in the bay for any specific storms (and we will discuss a counterexample below), but the range of peaks is higher in the bay. This finding is significant because, although it confirms previous findings related to storm surge sensitivities at the open coast (e.g., Musinguzi et al., 2021; Park & Youn, 2021; Shashank et al., 2021) and within

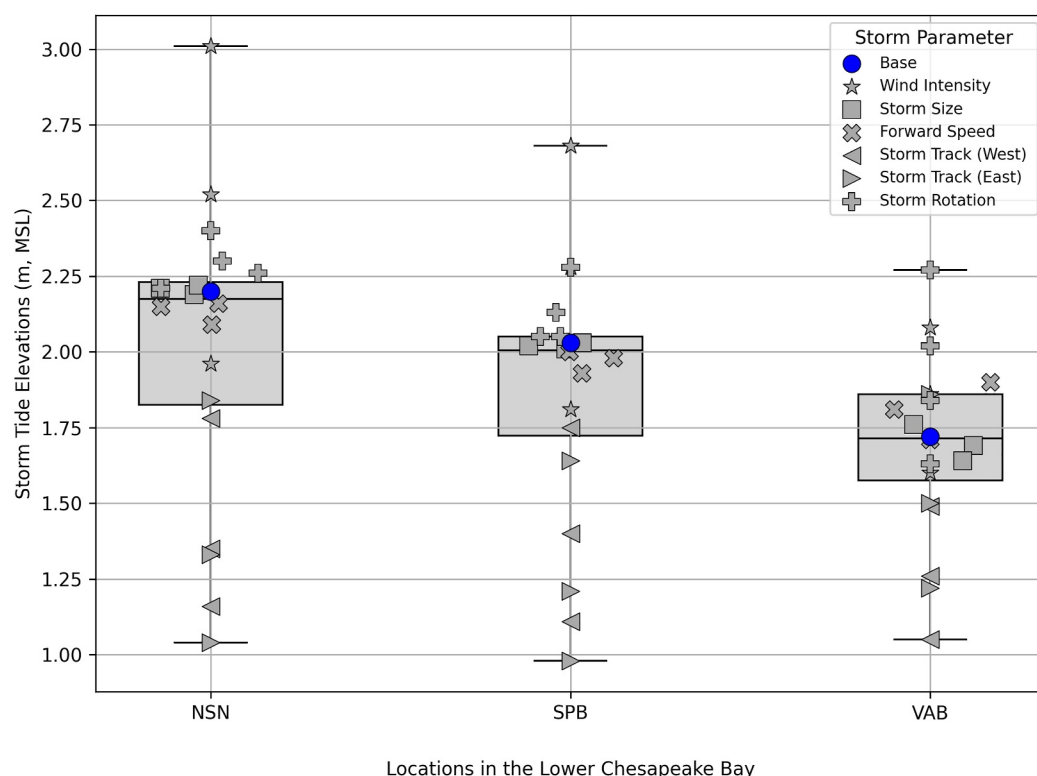


Figure 7. Peak storm tide variations from perturbations to the wind intensity (stars), storm sizes (squares), forward speeds (X crosses), track shifts (directional triangles for east and west), and angles of approach (plus crosses) at Naval Station Norfolk (NSN), Salt Pond Beach (SPB), and Virginia Beach (VAB). The study locations are shown from left to right representing the distance from the opening of the Chesapeake Bay. NSN is farthest away, while VAB is on the open coast. The base simulations are shown in blue circles for comparison. Some perturbation glyphs are jittered horizontally to reduce overlap.

bays (e.g., Bass et al., 2018; Du et al., 2020; Ramos-Valle et al., 2020; Weisburg & Zheng, 2006), we quantify the differences in peaks between the open coast and bay locations. At NSN, the range of 1.97 m was driven by the storms with wind magnitudes multiplied by 22.5%, where the peak storm tide was 3.01 m, and the storm shifted to the east by 255 km, where the peak was 1.04 m. At SPB, the range of 1.70 m was driven by the storms with wind magnitudes multiplied by 22.5%, where the peak storm tide was 2.68 m, and the storm shifted to the east by 255 km, where the peak was 0.98 m. At VAB, the range of 1.22 m was driven by the storms where the path of the storm was rotated by 75°, where the peak storm tide was 2.27 m and the storm shifted to the west by 255 km, where the peak was 1.05 m. This finding has implications for flood mitigation, because bay locations may need to be protected against a larger range of possible hazards, and for real-time forecasting, because uncertainties in storm predictions may translate into larger errors in flood predictions at bay locations.

Table 2

Summary of the Range of Storm Tides Produced From Perturbations of Irene to Each of the Storm Parameters Shown at Naval Station Norfolk, Salt Pond Beach, and Virginia Beach

Storm parameter	NSN	SPB	VAB
Wind Intensity	1.05	0.86	0.48
Storm Track (West)	1.04	0.92	0.67
Storm Track (East)	1.16	1.05	0.50
Storm Size	0.03	0.02	0.12
Forward Speed	0.07	0.07	0.19
Approach Angle	0.19	0.23	0.64

Note. The table shows expected trends for the wind intensity and storm track shifts to the east and west that align with the hypothesis. It also shows little to no changes in the range of storm tides from perturbations in the storm size and forward speed. However, it shows the approach angle with an opposing trend to the hypothesis.

The range of peak storm tides was most sensitive to the storm intensity and position relative to the region of interest. The maximum storm tides within the bay increased as the wind intensity increased. This result confirms earlier findings Musinguzi and Akbar (2021), who considered the individual and combined influence of wind intensity, surface pressure, and forward speed for Rita in 2005 over the southern coastal areas of Texas and Louisiana. Rising sea surface temperatures (Patricola & Wehner, 2018; Saba et al., 2016) contribute to stronger hurricanes (Colorado State University: Department of Atmospheric Science, 2024), and there

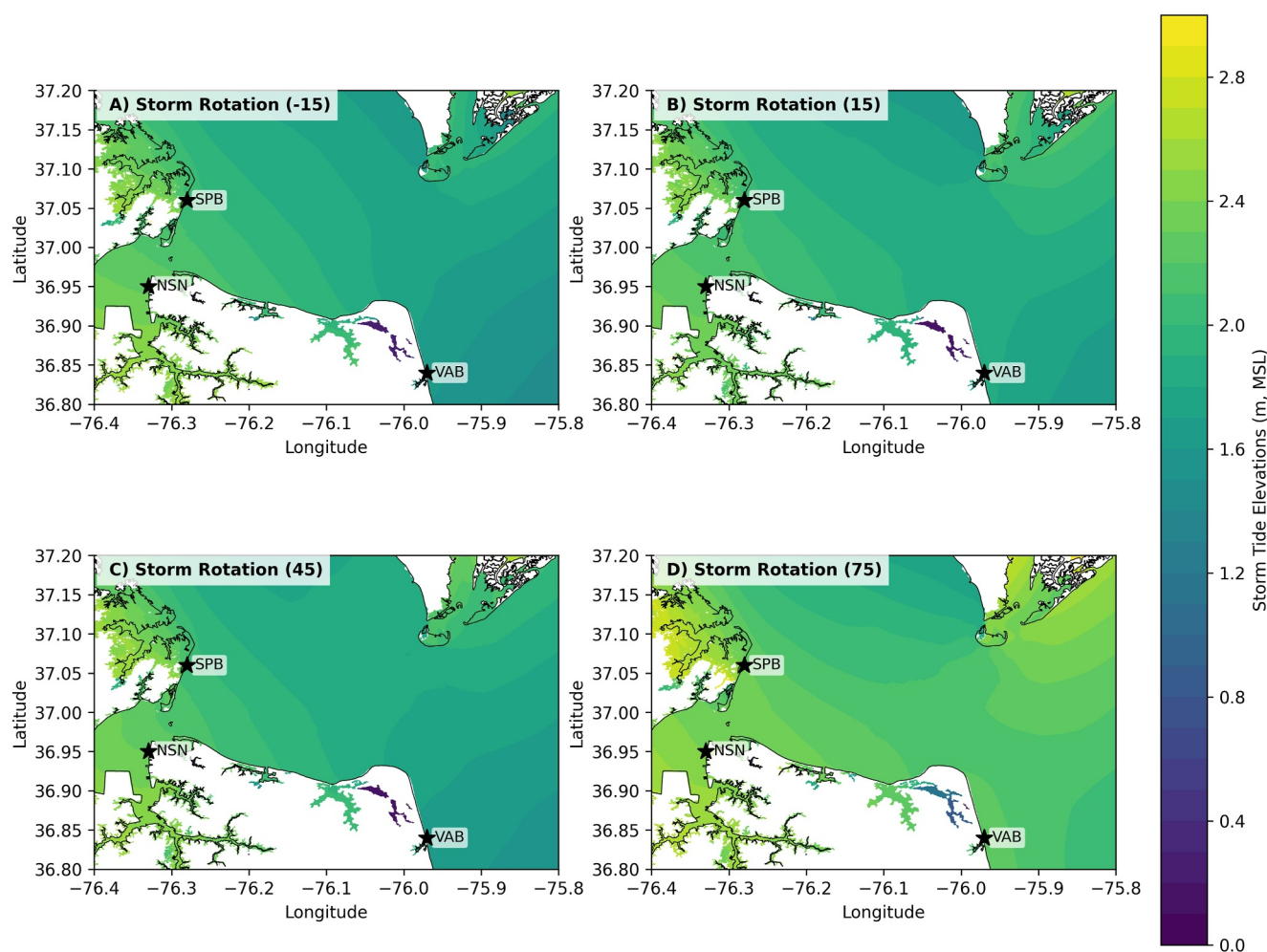


Figure 8. Spatial distribution of peak storm tides from the perturbations to the approach angles.

has been an increase in the frequency of Category-5 storms (Kossin et al., 2020). With stronger winds, these storms can cause devastating floods in coastal communities adjacent to bays. For example, storms like Ike in 2008 and Nicholas in 2021, which made landfalls as Category-2 and Category-1 storms, respectively, and affected the Galveston Bay, could have more severe impacts in the future.

The peak storm tide is also sensitive to changes in the storm's track to the east and west. As the perturbed storms made landfall closer to the bay, storm tides increased. This result confirms the findings of earlier studies (Ezer, 2018; Tsai et al., 2024), which shows that if the storm is too far offshore, the effects of storm tides are reduced, while if the storm is too far inland, the winds cannot fully develop storm tides over the body of water. Storm tides are greatest when the storm is close to the site of interest, and the winds are directed toward the coast. For example, Tampa Bay has experienced near misses of major catastrophes from storms like Ian in 2022 and Milton in 2024. Both storms made landfall just south of the bay and saw storm tides recede because of this effect. Had these storms made landfall farther north, Tampa Bay would have seen even more severe impacts.

A counterexample was observed in scenarios with perturbations of the storm's angle of approach. It was expected that, as the storm approached closer to shore-normal, 80° (Russo, 1998), the range of storm tides would increase from the base storm scenario and also from the open coast into the bay. However, while our results show an increase in peak storm tides due to the shore-normal track (confirming the results of Pandey & Rao, 2019), these scenarios show an increase in the range of peak storm tides at the coast as opposed to the bay locations. This trend is related to our point of rotation, which was selected as the location where Irene crossed back into the Atlantic. Close to the rotation point, such as at VAB, the winds changed significantly across the

scenarios, sometimes pushing water parallel to the coast (Figures 8a and 8b) and sometimes pushing water toward the coast (Figure 8d). Farther from the rotation point, such as SPB and NSN inside the bay, the storm surge was still controlled by the alignment of winds with the bay's major axis, and thus the storm tides did not vary as much, even when these locations were on the strong side of the perturbed track (Figure 8d). If a different point was selected for location, or if a smaller sheltered bay was considered, then the effects on the range of peak storm tides could be different.

5. Conclusion

Coastal communities near bays may be protected from the most intense waves and storm surges from offshore, but they may experience peak storm tides with more variation than at the open coast. The Lower Chesapeake Bay was affected by Irene in 2011, which caused flooding in the communities from the open coast (VAB) to the bay (Hampton, Norfolk). In this study, we used ADCIRC to assess the variation in ranges of peak storm tides within and around the Lower Chesapeake Bay. The major contributions and findings of this study can be summarized:

1. *The range of peak storm tides was larger at bay locations than at the open coast.* Across all storm scenarios, the range of peak storm tides increased from 1.22 m at VAB, to 1.70 m at SPB, and to 1.97 m at NSN, thus showing an increase of at least 47%. The IQRs also validate the hypothesis in that the ranges are smaller at the open coast (VAB, 0.28 m) and increase inside the bay (SPB, 0.33 m; NSN, 0.40 m). While these findings are specific for the Lower Chesapeake Bay, they may be applicable to other coastal water bodies with similar classifications, such as the Baltic Sea, Narragansett Bay, and the Hudson River, which have similar freshwater Froude number and mixing number (Geyer & MacCready, 2014).
2. *The wind intensity and storm track are significant contributors to the range of peak storm tides.* These parameters influence the upper and lower limits of the ranges, and they were mostly outside of the IQRs for all locations. At an inland location like a bay, small changes in these parameters could cause large changes in the storm tides at specific locations.
3. *Specific storms may still cause a larger peak storm tide at the open coast.* A counterexample was observed in scenarios of the storm's approach angle, which was perturbed by rotating around the location where Irene crossed back into the Atlantic. The strongest winds were aligned shore-parallel for some scenarios and shore-normal for other scenarios, causing significant differences in the peak storm tides at the VAB location. This result shows the sensitivity of the storm surge to the combined effects of the storm and coast.

Future work could include an examination of smaller, semienclosed bays closer to the open coast. This work would allow for a more comparative study to understand the impacts of those storm parameters from this study where little to no change was observed in the variation of storm tides. Another future work could also examine the worst-case scenario for possible storm tides within the region. While Irene was a historical storm that impacted this region, many possible storms of the future could be assessed to determine the magnitude of possible storm tides at any of the study locations to help surrounding communities plan for future hazards.

Conflict of Interest

The authors declare no conflicts of interest relevant to this study.

Data Availability Statement

The library of simulation data, including the unstructured finite element mesh, atmospheric forcings, and output files with time snaps of predicted storm tides, is available as a public archive (Knowles & Dietrich, 2025) in the Data Depot at DesignSafe-CI (Rathje et al., 2017).

References

- Amante, C. J., Love, M., Carignan, K., Sutherland, M. G., MacFerrin, M., & Lim, E. (2023). Continuously updated digital elevation models (CUDEMs) to support coastal inundation modeling. *Remote Sensing*, 15(6), 1702. <https://doi.org/10.3390/rs15061702>
- Avila, L. A., & Cangialosi, J. (2013). *Tropical cyclone report, Hurricane Irene (AL092011), 21–28 August 2011* (Technical Report). National Hurricane Center.
- Azad, A. A., & Marsooli, R. (2024). A high-resolution coupled circulation-wave model for regional dynamic downscaling of water levels and wind waves in the western north Atlantic Ocean. *Ocean Engineering*, 311, 118869. <https://doi.org/10.1016/j.oceaneng.2024.118869>
- Bass, B., Torres, J. M., Irza, J. N., Proft, J., Sebastian, A., Dawson, C., & Bedient, P. (2018). Surge dynamics across a complex bay coastline, Galveston Bay, TX. *Coastal Engineering*, 138, 165–183. <https://doi.org/10.1016/j.coastaleng.2018.04.019>

Acknowledgments

This work was supported by the Environmental Security Technology Certification Program (ESTCP; Project NH21-5028) under the U.S. Department of Defense. The authors are grateful for the feedback provided by Jens Figlus, Kees Nederhoff, Stephanie Patch, Ellen Quataert, Curt Storlazzi, and Ap van Dongeren during the development of this manuscript.

- Bilskie, M. V., & Luettich, R. A. (2024). The role of advection in storm surge for Hurricane Michael (2018). *Journal of Geophysical Research: Oceans*, 127(7), e2024JC021105. <https://doi.org/10.1029/2024JC021105>
- Blanton, B. O., Stillwell, L., Roberts, H., Atkinson, J., Zou, S., Forte, M. F., et al. (2011). *Coastal storm surge analysis: Computational system, report 2: Intermediate submission no. 1.2* (Technical Report No. TR-11-1). Renaissance Computing Institute. Retrieved from <https://apps.dtic.mil/sti/citations/ADA539306>
- Bowers, A. (2012). Looking back at Irene. <https://coastalreview.org/2012/08/looking-back-at-irene/>
- Bucci, L., Alaka, L., Hagen, A., Delgado, S., & Beven, J. (2023). *Tropical cyclone report for Hurricane Ian, 23 September – 30 September 2022* (Technical Report). National Hurricane Center.
- Camelo, J., Mayo, T., & Gutmann, E. (2020). Projected climate change impacts on hurricane storm surge inundation in the coastal United States. *Frontiers in Built Environment*, 6, 588049. <https://doi.org/10.3389/fbuil.2020.588049>
- Chesapeake Bay Foundation. (2024). Bay facts. Retrieved from <https://www.cbf.org/about-the-bay/bay-facts.html>
- Coastal Emergency Risks Assessment. (2024). Coastal emergency risks assessment. Retrieved from <https://cera.coastalrisk.live/>
- Cobell, Z. (2020). ADCIRCModules: A C++ and Python interface for manipulation of ADCIRC model data. <https://github.com/zcobell/ADCIRCModules>
- Colorado State University: Department of Atmospheric Science. (2024). North Atlantic Ocean historical tropical cyclone statistics. Retrieved from <https://tropical.atmos.colostate.edu/Realtime/index.php?arch&loc=northatlantic>
- Cyriac, R., Dietrich, J. C., Fleming, J. G., Blanton, B. O., Kaiser, C., Dawson, C. N., & Luettich, R. A. (2018). Variability in coastal flooding predictions due to forecast errors during Hurricane Arthur (2014). *Coastal Engineering*, 137, 59–78. <https://doi.org/10.1016/j.coastaleng.2018.02.008>
- Danso, D. K., & Patricola, C. M. (2024). Future projections of storm surge in Hurricane Katrina and sensitivity to meteorological forcing resolution. *Environmental Research Communications*, 6(9), 095018. <https://doi.org/10.1088/2515-7620/ad7351>
- Dietrich, J. C., Muhammad, A., Curcic, M., Fathi, A., Dawson, C. N., Chen, S. S., & Luettich, R. A. (2018). Sensitivity of storm surge predictions to atmospheric forcing during Hurricane Isaac. *Journal of Waterway, Port, Coastal, and Ocean Engineering*, 144(1), 04017035. [https://doi.org/10.1061/\(asce\)ww.1943-5460.0000419](https://doi.org/10.1061/(asce)ww.1943-5460.0000419)
- Dietrich, J. C., Westerink, J. J., Kennedy, A. B., Smith, J. M., Jensen, R. E., Zijlema, M., et al. (2011). Hurricane Gustav (2008) waves and storm surge: Hindcast, validation and synoptic analysis in southern Louisiana. *Monthly Weather Review*, 139(8), 2488–2522. <https://doi.org/10.1175/2011mwr3611.1>
- Du, M., Hou, Y., Hu, P., & Wang, K. (2020). Effects of typhoon paths on storm surge and coastal inundation in the Pearl River Estuary, China. *Remote Sensing*, 12(11), 1851. <https://doi.org/10.3390/rs12111851>
- Egbert, G. D., & Erofeeva, S. Y. (2002). Efficient inverse modeling of Barotropic Ocean tides. *Journal of Atmospheric and Oceanic Technology*, 19(2), 183–204. [https://doi.org/10.1175/1520-0426\(2002\)019<0183:eimobo>2.0.co;2](https://doi.org/10.1175/1520-0426(2002)019<0183:eimobo>2.0.co;2)
- Emmanuel, K. (1987). The dependence of hurricane intensity on climate. *Nature*, 326(6112), 483–485. <https://doi.org/10.1038/326483a0>
- Ezer, T. (2018). The increased risk of flooding in Hampton Roads: On the roles of sea level rise, storm surges, hurricanes, and the gulf stream. *Marine Technology Society Journal*, 52(2), 34–44. <https://doi.org/10.4031/MTSJ.52.2.6>
- Ezer, T. (2019). Numerical modeling of the impact of hurricanes on ocean dynamics: Sensitivity of the gulf stream response to storm's track. *Ocean Dynamics*, 69(9), 1053–1066. <https://doi.org/10.1007/s10236-019-01289-9>
- Ezer, T., Henderson-Griswold, S., & Updyke, T. (2022). Dynamic observations in the Hampton Roads region: How surface currents at the mouth of Chesapeake Bay may be linked with winds, water level, river discharge and remote forcing from the gulf stream. In *Oceans 2022, Hampton Roads*. <https://doi.org/10.1109/OCEANS47191.2022.9977092>
- Fahad, M. G. R., & Nazari, R. (2021). Development of a decision support framework for multi-hazard resilience assessment of coastal structures. In *Geo-extreme 2021* (pp. 318–328). <https://doi.org/10.1061/9780784483688.032>
- FEMA. (2021). Flood risk study engineering library. Retrieved from <https://hazards.fema.gov/wps/portal/frisel>
- Fosell, K., Ahijevych, D., Morss, R., Snyder, C., & Davis, C. (2017). The practical predictability of storm tide from tropical cyclones in the Gulf of Mexico. *American Meteorological Society*, 45, 5103–5121. <https://doi.org/10.1175/MWR-D-17-0051.1>
- Gao, J. (2018). *On the surface wind stress for storm surge modeling*. University of North Carolina at Chapel Hill. <https://doi.org/10.17615/zpeb-7k73>
- Garzon, J. L., & Ferreira, C. M. (2016). Storm surge modeling in large estuaries: Sensitivity analyses to parameters and physical processes in the Chesapeake Bay. *Journal of Marine Science and Engineering*, 4(3), 1–32. <https://doi.org/10.3390/jmse4030045>
- Geyer, W. R., & MacCready, P. (2014). The estuarine circulation. *Annual Review of Fluid Mechanics*, 46, 175–197.
- Hallock, Z. R., Pistek, P., Book, J. W., Miller, J. L., Shay, L. K., & Perkins, H. T. (2003). A description of tides near the Chesapeake Bay entrance using in situ data with an adjoint model. *Journal of Geophysical Research*, 108(C3), 3075. <https://doi.org/10.1029/2001JC000820>
- Hoffman, R. N., & Gombos, D. (2012). Hurricane irene (2011) “worst-case” estimates of wind damage to property from exigent analysis of ecmwf ensemble forecasts. *Geophysical Research Letters*, 39(16), L16802. <https://doi.org/10.1029/2012GL052646>
- Holland, R. W. (1980). An analytic model of the wind and pressure profiles in hurricanes. *Monthly Weather Review*, 108(8), 1212–1218. [https://doi.org/10.1175/1520-0493\(1980\)108<1212:aamotw>2.0.co;2](https://doi.org/10.1175/1520-0493(1980)108<1212:aamotw>2.0.co;2)
- Hope, M. E., Westerink, J. J., Kennedy, A. B., Kerr, P. C., Dietrich, J. C., Dawson, C. N., et al. (2013). Hindcast and validation of hurricane ike (2008) waves, forerunner, and storm surge. *Journal of Geophysical Research: Oceans*, 118(9), 4424–4460. <https://doi.org/10.1002/jgrc.20314>
- Irish, J. L., Resio, D. T., & Ratcliff, J. J. (2008). The influence of storm size on hurricane surge. *Journal of Physical Oceanography*, 38(9), 2003–2013. <https://doi.org/10.1175/2008jpo3727.1>
- Islam, M. R., Lee, C., Mandi, K. T., & Takagi, H. (2021). A new tropical cyclone surge index incorporating the effects of coastal geometry, bathymetry and storm information. *Scientific Reports*, 11(1), 16747. <https://doi.org/10.1038/s41598-021-95825-7>
- Kerns, B. W., & Chen, S. (2023). Compound effects of rain, storm surge, and river discharge on coastal flooding during Hurricane Irene and Tropical Storm Lee (2011) in the Mid-Atlantic region: Coupled atmosphere-wave-ocean model simulation and observations. *Natural Hazards*, 116(1), 693–726. <https://doi.org/10.1007/s11069-022-05694-0>
- Kerr, P. C., Martyr, R. C., Donahue, A. S., Hope, M. E., Westerink, J. J., Luettich Jr, R. A., et al. (2013). US IOOS coastal and ocean modeling testbed: Evaluation of tide, wave, and hurricane surge response sensitivities to mesh resolution and friction in the Gulf of Mexico. *Journal of Geophysical Research: Oceans*, 118(9), 4633–4661. <https://doi.org/10.1002/jgrc.20305>
- Khalid, A., Miesse, T., Erfani, E., Thomas, S., Ferreira, C., Pegion, K., et al. (2021). Evaluating storm surge predictability on subseasonal timescales for flood forecasting applications: A case study for Hurricane Isabel and Katrina. *Weather and Climate Extremes*, 34, 100378. <https://doi.org/10.1016/j.wace.2021.100378>
- Kinnmark, I. (1986). The shallow water wave equations: Formulation, analysis and application. In C. A. Brebbia & S. A. Orszag (Eds.), *Lecture notes in engineering* (Vol. 15, pp. 12–26). Springer-Verlag.

- Knowles, J. S., & Dietrich, J. C. (2025). Library of ranges of peak storm tides between open-coast and bay locations. <https://doi.org/10.17603/ds2-r6x4-yy22>
- Kossin, J. P., Knapp, K. P., Olander, T. L., & Velden, C. S. (2020). Global increase in major tropical cyclone exceedance probability over the past four decades. *Proceedings of the National Academy of Sciences of the United States of America*, *117*(22), 11975–11980. <https://doi.org/10.1073/pnas.1920849117>
- Lee, S. B., Li, M., & Zhang, F. (2017). Impact of sea level rise on tidal range in Chesapeake and Delaware bays. *Journal of Geophysical Research: Oceans*, *122*(5), 3917–3938. <https://doi.org/10.1002/2016JC012597>
- Li, J., Hou, Y., Mo, D., Liu, Q., & Zhang, Y. (2019). Influence of tropical cyclone intensity and size on storm surge in the northern East China Sea. *Remote Sensing*, *11*(24), 3033. <https://doi.org/10.3390/rs11243033>
- Li, M., Zhong, L., Boicourt, W. C., Zhnag, A., & Zhang, D. (2006). Hurricane-induced storm surges, currents and destratification in a semi-enclosed Bay. *Geophysical Research Letters*, *33*, L02604. <https://doi.org/10.1029/2005GL024992>
- Little, C. M., Hu, A., Hughes, C. W., McCarthy, G. D., Piecuch, C. G., Ponte, R. M., & Thomas, M. D. (2019). The relationship between U.S. East Coast sea level and the Atlantic meridional overturning circulation: A review. *Journal of Geophysical Research: Oceans*, *124*(9), 6435–6458. <https://doi.org/10.1029/2019JC015152>
- Luettich, R. A., & Westerink, J. J. (2004). Formulation and numerical implementation of the 2D/3D ADCIRC finite element model version 44.XX. Retrieved from https://adcirc.org/files/2018/11/adcirc_theory_2004_12_08.pdf
- Luettich, R. A., Westerink, J. J., & Scheffner, N. W. (1992). ADCIRC: An advanced three-dimensional circulation model for shelves coasts and estuaries, report 1: Theory and methodology of ADCIRC-2DDI and ADCIRC-3DL (Technical Report). *United States Army Corps of Engineers*. https://www.researchgate.net/publication/235019369_ADCIRC_An_Advanced_Three-Dimensional_Circulation_Model_for_Shelves_Coasts_and_Estuaries_Report_1_Theory_and_Methodology_of_ADCIRC-2DDI_and_ADCIRC-3DL
- Marley, R. (2017). Largest naval bases in the world. <https://vocal.media/serve/largest-naval-bases-in-the-world>. (Retrieved 15 October 2024).
- Mousavi, M. R., Irish, J. L., Frey, A. E., Olivera, F., & Edge, B. L. (2011). Global warming and hurricanes: The potential impact of hurricane intensification and sea level rise on coastal flooding. *Climatic Change*, *104*(3–4), 575–597. <https://doi.org/10.1007/s10584-009-9790-0>
- Musinguzi, A., & Akbar, M. K. (2021). Effect of varying wind intensity, forward speed, and surface pressure on storm surges of Hurricane Rita. *Journal of Marine Science and Engineering*, *9*(2), 128–148. <https://doi.org/10.3390/jmse9020128>
- Musinguzi, A., Shamsu, M., Akbar, M. K., & Fleming, J. G. (2021). Understanding the effects of wind intensity, forward speed, pressure and track on generation and propagation of Hurricane Irma surges around Florida. *Journal of Marine Science and Engineering*, *9*, 963–986. <https://doi.org/10.3390/jmse9090963>
- National Hurricane Center. (2011). Atcf archives. Retrieved from <https://ftp.nhc.noaa.gov/atcf/archive/2011/>
- National Oceanic and Atmospheric Administration. (2011). Hurricane Irene (Technical Report). Retrieved from <https://repository.library.noaa.gov/view/noaa/17128>
- National Oceanic and Atmospheric Administration. (2024a). *National Oceanic and atmospheric administration*. National Ocean Service. Retrieved from <https://oceanservice.noaa.gov/facts/stormsurge-stormtide.html>
- National Oceanic and Atmospheric Administration. (2024b). Tides and currents. Retrieved from <https://tidesandcurrents.noaa.gov/>
- National Oceanic and Atmospheric Administration, Office for Coastal Management. (2016). 2016 coastal change analysis program (c-cap) regional land cover. Retrieved from www.coast.noaa.gov/htdata/raster/landcover/bulkdownload/30m_lc/
- National Weather Service. (2022). The hurricane history of central and eastern Virginia. Retrieved from <https://www.weather.gov/media/akq/miscNEWS/hurricanehistory.pdf>
- National Weather Service. (2025a). Hurricane Katrina - A look back 15 years later. Retrieved from https://www.weather.gov/lix/katrina_anniversary#:~:text=Storm%20Impact%20A%20very%20large%20storm%20surge,where%20storm%20surge%20heights%20approached%2028%20feet
- National Weather Service. (2025b). Tropical cyclone report. Retrieved from https://www.nhc.noaa.gov/data/tcr/AL092008_Ike.pdf
- Owensby, M., Bryant, M., Provost, L., Hesser, T., Massey, T. C., Tritinger, A., & Ding, Y. (2020). *Calibration and validation of the south Atlantic domain model setup for the south Atlantic coastal study (SACS)* (Technical Report). US Army Corps of Engineers.
- Pandey, S., & Rao, A. (2019). Impact of approach angle of an impinging cyclone on generation of storm surges and its interaction with tides and wind waves. *Journal of Geophysical Research: Oceans*, *124*(11), 7643–7660. <https://doi.org/10.1029/2019JC015433>
- Park, Y. H., & Youn, D. (2021). Characteristics of storm surge based on the forward speed of the storm. *Journal of Coastal Research*, *114*(sp1), 71–75. <https://doi.org/10.2112/JCR-S1114-015.1>
- Patricola, C. M., & Wehner, M. F. (2018). Anthropogenic influences on major tropical cyclone events. *Nature*, *563*(7731), 339–346. <https://doi.org/10.1038/s41586-018-0673-2>
- Qian, X., Hwang, S., & Son, S. (2024). A study on key determinants in enhancing storm surges along the coast: Interplay between tropical cyclone motion and coastal geometry. *Journal of Geophysical Research: Oceans*, *129*, 1–2. <https://doi.org/10.1029/2023JC020400>
- Ramos-Valle, A., Curchitser, E., & Bruyere, C. (2020). Impact of tropical cyclone landfall angle on storm surge along the Mid-Atlantic Bight. *Journal of Geophysical Research: Atmospheres*, *125*(4), e2019JD031796. <https://doi.org/10.1029/2019JD031796>
- Rathje, E., Dawson, C. N., Padgett, J. E., Pinelli, J.-P., Stanzione, D., Adair, A., et al. (2017). DesignSafe: A new cyberinfrastructure for natural hazards engineering. *ASCE Natural Hazards Review*, *18*(3), 06017001. [https://doi.org/10.1061/\(ASCE\)NH.1527-6996.0000246](https://doi.org/10.1061/(ASCE)NH.1527-6996.0000246)
- Rego, J. L., & Li, C. (2009). On the importance of the forward speed of hurricanes in storm surge forecasting: A numerical study. *Geophysical Research Letters*, *36*(7), L07609. <https://doi.org/10.1029/2008gl036953>
- Rego, J. L., & Li, C. (2010). Storm surge propagation in Galveston Bay during Hurricane Ike. *Journal of Marine Systems*, *82*(4), 265–279. <https://doi.org/10.1016/j.jmarsys.2010.06.001>
- Roberts, K. J., Pringle, W. J., & Westerink, J. J. (2019). OceanMesh2D 1.0: MATLAB-based software for two-dimensional unstructured mesh generation in coastal ocean modeling. *Geoscientific Model Development*, *12*(5), 1847–1868. <https://doi.org/10.5194/gmd-12-1847-2019>
- Russo, E. P. (1998). Estimating hurricane storm surge amplitudes for the Gulf of Mexico and Atlantic coastlines of the United States. *IEEE Oceanic Engineering Society*, *3*, 1301–1305. <https://doi.org/10.1109/OCEANS.1998.726278>
- Saba, V. S., Griffies, S. M., Anderson, W. G., Winton, M., Alexander, M. A., Delworth, T. L., et al. (2016). Enhanced warming of the northwest Atlantic Ocean under climate change. *Journal of Geophysical Research: Oceans*, *121*(1), 118–132. <https://doi.org/10.1002/2015JC011346>
- Sadri, A. M., Ukkusuri, S., Murray-Tuite, P., & Gladwin, H. (2015). Hurricane evacuation route choice of major bridges in Miami Beach, Florida. *Transportation Research Record: Journal of the Transportation Research Board*, *2532*(1), 164–173. <https://doi.org/10.3141/2532-18>
- Salehi, M. (2018). Storm surge and wave impact of low-probability hurricanes on the lower Delaware Bay - Calibration and application. *Journal of Marine Science and Engineering*, *6*(2), 54. <https://doi.org/10.3390/jmse6020054>
- Salisbury, M. B., & Hagen, S. C. (2007). The effect of tidal inlets on open coast storm surge hydrographs. *Coastal Engineering*, *54*(5), 377–391. <https://doi.org/10.1016/j.coastaleng.2006.10.002>

- Sebastian, A. G., Proft, J. M., Dietrich, J. C., Du, W., Bedient, P. B., & Dawson, C. N. (2014). Characterizing hurricane storm surge behavior in Galveston Bay using the SWAN+ADCIRC model. *Coastal Engineering*, 88, 171–181. <https://doi.org/10.1016/j.coastaleng.2014.03.002>
- Sebastian, M., Behera, M. R., & Murty, P. L. (2019). Storm surge hydrodynamics at a concave Coast due to varying approach angles of cyclone. *Ocean Engineering*, 191, 106437. <https://doi.org/10.1016/j.oceaneng.2019.106437>
- Shashank, V. G., Mandal, S., & Sil, S. (2021). Impact of varying landfall time and cyclone intensity on storm surges in the Bay of Bengal using ADCIRC model. *Journal of Earth System Science*, 130(4), 194. <https://doi.org/10.1007/s12040-021-01695-y>
- Shashank, V. G., Sriram, V., Schuttrumpf, H., & Sannasiraj, S. A. (2024). A new surge index with the incorporation of cyclone track approach angle information for the Bay of Bengal. *Coastal Engineering*, 188, 104429. <https://doi.org/10.1016/j.coastaleng.2023.104429>
- Shi, W., Wang, M., & Jiang, L. (2013). Tidal effects on ecosystem variability in the Chesapeake Bay from modis-aqua. *Remote Sensing of Environment*, 138, 65–76. <https://doi.org/10.1016/j.rse.2013.07.002>
- Sichani, M. E., Anarde, K., Capshaw, K., Meidl, R., Hassanzadeh, P., Loch, T., & Bedient, P. (2020). Hurricane risk assessment of petroleum infrastructure in a changing climate. *Frontiers in Built Environment*, 6, 104. <https://doi.org/10.3389/fbuil.2020.00104>
- Stark, J., Oyen, T. V., Meire, P., & Temmerman, S. (2015). Observations of tidal and storm surge attenuation in a large tidal marsh. *Limnology & Oceanography*, 60(4), 1371–1381. <https://doi.org/10.1002/lno.10104>
- Thomas, A., Dietrich, J. C., Asher, T. G., Blanton, B. O., Cox, A. T., Dawson, C. N., et al. (2019). Influence of storm timing and forward speed on tide-surge interactions during Hurricane Matthew. *Ocean Modelling*, 137, 1–19. <https://doi.org/10.1016/j.ocemod.2019.03.004>
- Tsai, Y., Wu, T., Yen, E., Tanpipat, V., & Lin, C. (2024). Storm surge induced by Tropical Storm Pabuk (2019) and its impact by track variation scenarios on the Thailand coast. *Natural Hazards*, 120(14), 13009–13039. <https://doi.org/10.1007/s11069-024-06717-8>
- U.S. Army Corps of Engineers. (2013). *Coastal storm surge analysis: Modeling system validation* (Technical Report). U.S. Army Corps of Engineers.
- U.S. Geological Survey. (2016). Location matters: Sandy's tides hit some parts of the new Jersey coast harder than others. Retrieved from [https://www.usgs.gov/news/state-news-release/location-matters-sandys-tides-hit-some-parts-new-jersey-coast-harder-others#:~:text=The%20researchers%20found%20that%20peak%20storm%20tide,ranged%20from%20about%205%20to%208%20feet./](https://www.usgs.gov/news/state-news-release/location-matters-sandys-tides-hit-some-parts-new-jersey-coast-harder-others#:~:text=The%20researchers%20found%20that%20peak%20storm%20tide,ranged%20from%20about%205%20to%208%20feet/)
- U.S. Geological Survey. (2018). U.S. Geological Survey. Retrieved from <https://www.usgs.gov/centers/eros/science/usgs-eros-archive-digital-elevation-shuttle-radar-topography-mission-srtm-1>
- Weisburg, R. H., & Zheng, L. (2006). Hurricane storm surge simulations for Tampa Bay. *Estuaries and Coasts*, 29(6), 899–913. <https://doi.org/10.1007/BF02798649>
- Westerink, J. J., Luettich Jr, R. A., Feyen, J. C., Atkinson, J. H., Dawson, C. N., Roberts, H. J., et al. (2008). A Basin to channel Scale unstructured grid hurricane storm surge model applied to Southern Louisiana. *Monthly Weather Review*, 136(3), 833–864. <https://doi.org/10.1175/2007mwr1946.1>
- Yang, K., Davidson, R. A., Vergara, H., Kolar, R. L., Dresback, K. M., Colle, B. A., et al. (2019). Incorporating inland flooding into hurricane evacuation decision support modeling. *Natural Hazards*, 96(2), 857–878. <https://doi.org/10.1007/s11069-019-03573-9>
- Zhang, F., & Li, M. (2019). Impacts of ocean warming, sea level rise, and coastline management on storm surge in a semienclosed Bay. *Journal of Geophysical Research: Oceans*, 124(9), 6498–6514. <https://doi.org/10.1029/2019JC015445>
- Zhang, Z., Guo, F., Song, Z., Chen, P., Liu, F., & Zhang, D. (2022). A numerical study of storm surge behavior in and around Lingdingyang Bay, Pearl River estuary, China. *Natural Hazards*, 111(2), 1507–1532. <https://doi.org/10.1007/s11069-021-05105-w>